SUPPLEMENTARY MATERIAL

Hypokalemia promotes arrhythmia by distinct mechanisms in atrial and ventricular myocytes

Kiarash Tazmini,[1,2*] Michael Frisk,[1,3*] Alexandre Lewalle,[4] Martin Laasmaa,[1,3] Stefano Morotti,[5] David B. Lipsett,[1] Ornella Manfra,[1,3] Jonas Skogested,[1] Jan M. Aronsen,[1,6] Ole M. Sejersted,[1] Ivar Sjaastad,[1,3] Andrew G. Edwards,[5] Eleonora Grandi,[5] Steven A. Niederer,[4] Erik Øie,[2] and William E. Louch[1,3]

[1] Institute for Experimental Medical Research, Oslo University Hospital and University of Oslo, Oslo, Norway

[2] Department of Internal Medicine, Diakonhjemmet Hospital, Oslo, Norway

[3] KG Jebsen Center for Cardiac Research, University of Oslo, Oslo, Norway

[4] Division of Imaging Sciences and Biomedical Engineering, King's College London, London, UK

[5] Department of Pharmacology, School of Medicine, University of California Davis, Davis, CA, USA

[6] Bjørknes College, Oslo, Norway

* These authors contributed equally to this manuscript

EXPANDED METHODS

Ethical approval

This study was approved by the Norwegian Animal Research Authority (FDU application number 7786) under the Norwegian Animal Welfare Act, and conformed with Directive 2010/63/EU of the European Parliament.

Isolation of ventricular cardiomyocytes

Male Wistar rats (~10 weeks old and ~300 g) were housed in a temperature-regulated room with 12 h day/12 h night cycling, and free access to food and water. Rats were sedated with a mixture of 5% isoflurane and 95% O_2, and sacrificed by cervical dislocation. Excised hearts were placed in cool, oxygenated buffer solution containing (in mM): NaCl 130, KCl 5.4, $MgCl_2$ 0.5, NaH_2PO_4 0.4, Hepes 25, D-glucose 5.5, pH=7.4 with NaOH, and ~ 5000 IU heparin. The excised heart was rapidly cannulated and mounted on a Langendorff setup, and retrogradely perfused through the aorta with the oxygenated buffer solution described above at 37°C. When the heart was cleared of blood, the perfusion was switched to buffer solution supplemented with 200 U/ml collagenase type II (Worthington Biochemical, Lakewood, NJ, USA) and 0.04 mM Ca^{2+} for 18-20 min. The right and left atria were then carefully excised and stored in cold buffer for further digestion and isolation of atrial cardiomyocytes (see

below). The left ventricle was cut down, minced, and gently triturated with a cutoff Pasteur pipette for ~1 min in collagenase-free buffer containing 1% bovine serum albumin (BSA) (Sigma Aldrich, St. Louis, MO, USA) and ~0.02 U/ml deoxyribonuclease I (Worthington Biochemical Corporation, Lakewood, NJ, USA). The cell-containing solution was then filtered through 200-µm nylon mesh, and Ca^{2+} concentration was progressively increased (0.1, 0.2, and 0.5 mM). The isolated ventricular myocytes were stored at room temperature and used in experiments within 10 h of isolation.

Isolation of atrial cardiomyocytes

A secondary digestion of the excised atria was performed as previously described.[12] Each atrium was cut into small pieces (~1 mm^3) with a sharp razor blade, and gently agitated in a spinner-bottle containing (in mM): NaCl 100, KCl 10, $MgSO_4$ 5, KH_2PO_4 1, $CaCl_2$ 0.02, Hepes 5, D-glucose 20, Taurin10, 0.5 % BSA, and pH =7.4. 400 U/mL of collagenase type II (Worthington Biochemical Corporation) was added to facilitate further digestion. After 20 min, the tissue chunks were washed with clean solution, and gently triturated with a Pasteur pipette for ~2 min with addition of ~0.02 U/mL deoxyribonuclease I (Worthington Biochemical). The isolated atrial myocytes were then filtered through 200-µm nylon mesh, sedimented, and washed with clean buffer containing increasing Ca^{2+} concentrations (0.1, 0.2, and 0.5 mM). Right and left atria myocytes were maintained separately at room temperature, and studied within 10 h of isolation.

Recordings of Ca^{2+} transients and waves

Ca^{2+} transients were recorded in isolated atrial and ventricular myocytes loaded with 20 µM fluo-4 AM (Molecular Probes, Eugene, OR, USA) for 10 min. Cells were plated on laminin-coated coverslips, and placed in a superfusion chamber mounted on an inverted microscope. Characterization of whole-cell Ca^{2+} transients was performed in cells which were field-stimulated at 1 Hz through two platinum electrodes with 3 ms biphasic pulses, 25% above threshold. Fluo-4 was excited at 485 nm and emitted light >510 nm was registered with a photomultiplier tube (Photon Technology International, Monmouth Junction, NJ, USA). Ca^{2+} transients were recorded during an initial 2 min control period, when myocytes were superfused at 37°C with a solution containing (in mM): NaCl 140, KCl 5.0, $MgCl_2$ 0.5, NaH_2PO_4 0.4, $CaCl_2$ 1.0, Hepes 5, D-glucose 5.5, pH adjusted to 7.4 with NaOH. Hypokalemia was then simulated by rapidly reducing $[K^+]_o$ from 5.0 mM to 2.7 mM via a

rapid-solution changer for the ensuing 3 min. This protocol was conducted for only one cardiomyocyte per plate.

In follow-up experiments, the incidence of Ca^{2+} waves was investigated during a 30 s pause in the stimulation, performed after 2 min of stable Ca^{2+} transient recordings in $[K^+]_o$ = 5.0 mM, and then again after 3 min in $[K^+]_o$ = 2.7 mM.

SR Ca^{2+} content was estimated by rapid application of 10 mM caffeine (Sigma-Aldrich), and measuring the magnitude of the resulting Ca^{2+} transient. Ca^{2+} transients elicited by 1 Hz field stimulation during continuous caffeine superfusion were employed to examine rates of Ca^{2+} extrusion, using exponential fits of the decay phase of each transient.[16]

In a subset of experiments, Ca^{2+} transients were examined with inclusion of 0.3 µmol/L ouabain (Sigma-Aldrich) in the normokalemic and hypokalemic solutions, to allow preferential inhibition of the α2 NKA isoform.[19]

Recordings of Ca^{2+} transients, waves, and caffeine responses were analyzed with Clampfit 9.0 (Axon Instruments, Foster City, CA, USA). Ca^{2+} transient magnitudes are presented as peak fluorescence values normalized to resting fluorescence (F/F_0). Representative recordings were smoothed with a moving average or Savitzky-Golay filter in TableCurve 2D (Systat Software Inc, Chicago, USA).

T-tubule imaging in isolated cardiomyocytes

Initial quantification of t-tubule structure in isolated ventricular and atrial myocytes was performed by staining cells with 10 µmol/L di-8-ANEPPS (Invitrogen, Paisley, UK) for 20 min. Plated cells were then scanned longitudinally along their central axis, using a confocal microscope (LSM 710, Zeiss, Jena, Germany, pinhole=0.9 µm) with a 60x objective. Di-8-ANEPPS was excited at 488 nm, and emission was measured above 510 nm. 2048×2048 pixel images were deconvolved using Huygens Essential software (Scientific Volume Imaging, Hilversum, The Netherlands), and a point spread function calculated from images of 100 nm-diameter fluorescent beads (Microprobes, Gaithersburg, MD). For each cell, t-tubule density was determined by thresholding the image intensity of the entire cell by the Otsu method, using an automated algorithm in ImageJ (National Institutes of Health). The t-index[17] was then calculated for the myocyte interior, defined as the percentage of the cellular cross-

sectional area, excluding the nucleus, occupied by above-threshold pixels. Cells exhibiting a t-index of ≥ 2% were defined as being tubulated, which roughly corresponds to the level detectable by eye.[12]

In follow-up experiments, t-tubule labeling was paired with Ca^{2+} imaging and/or electrophysiological measurements. T-tubules were stained with di-8-ANEPPS, as above, or with CellMask Orange (1:1000 dilution; Thermo Fisher Scientific, Waitham, MA, USA; C10045) for 10 min. CellMask Orange was excited at 546 nm, and emission was measured above 560 nm. Confocal images were obtained with an LSM 510 confocal microscope (Zeiss), with a 40x objective and pinhole set to 1 Airy unit (80 µm).

Monitoring of intracellular Na^+

Intracellular Na^+ levels were assessed in myocytes loaded with SBFI AM (Thermo Fischer) and 0.15% Pluronic F-127 for 45 min.[16, 19] Cardiomyocytes were field stimulated and superfused with the same normokalemic and hypokalemic solutions as used in the fluo-4 experiments (1 Hz pacing, 37ºC). The sensitivity of SBFI to detect changes in intraclleular $[Na^+]$ was examined by permeabilizing ventricular cardiomyocytes with 2 µg/mol monensin and 30 µmol/L gramicidin (both Sigma-Aldrich),[16, 19] and then perfusing with progressively increasing Na^+ concentrations spanning the physiological range. SBFI was excited at 340 nm and emission measured at 410 and 590 nm. Results are presented as an emission ratio (410/590).

Detubulation

Ventricular cardiomyocytes were detubulated using a protocol similar to that described by Kawai *et al.*[18] Myocytes were added to a Hepes Tyrodes solution containing (in mM): NaCl 140.0, KCl 5.4, $MgCl_2$ 0.5, NaH_2PO_4 0.4, Hepes 5.0, D-Glucose 5.5, $CaCl_2$ 1.0, pH 7.4 with NaOH. Osmotic shock was induced by adding 1.5 mM formamide (Sigma-Aldrich, F5786), and placing the cell suspension on a shaker for 15 min at room temperature. The cells were then pelleted by centrifugation at 500 rpm for 30 s, and resuspended in HEPES Tyrodes solution to remove the formamide. After 5 min of incubation on a cell shaker (5 min, room temperature), cells were washed once more by centrifugation and resuspension. Successful detubulation was verified by di-8-ANNEPS staining and confocal imaging, as above. Ca^{2+} transients were then examined by wide-field fluo-4 fluorescence during 1 Hz field stimulation, as described.

Fixation, immunocytochemistry, and imaging of isolated myocytes

8-well LAB-TEK® chambered coverglasses (Thermo Fisher; 155411) were coated with 0.01% poly-L lysine solution (Sigma-Aldrich) for 15 min at room temperature, followed by coating overnight with 10 µg/ml natural mouse laminin (Thermo Fisher) in Medium 199 (Thermo Fisher). Isolated adult cardiomyocytes were seeded on coated coverglasses for 30-45 min, prior to fixation with 4% paraformaldehyde in ventricular myocyte isolation buffer (see above) for 5 min at room temperature. Cells were subsequently washed with PBS and fixation was quenched with 100 mM glycine solution in PBS. Membranes were permeabilized with 0.5% Triton X-100 (Sigma-Aldrich) in PBS and non-specific antigens were blocked by incubating in a solution containing 15.1 mM NaCl, 1.75 mM $Na_3C_6H_5O_7$, 5% normal goat serum, 3% BSA and 0.02% NaN_3 for 2 h at room temperature. Primary and secondary antibodies were diluted in a solution containing 15.1 mM NaCl, 1.75 mM $Na_3C_6H_5O_7$, 2% normal goat serum, 1% BSA and 0.02% NaN_3 and applied to cells overnight at 4°C and for 2 h at room temperature, respectively. Cells were washed with PBS between most steps following fixation, but not prior to incubation with primary antibody. Finally, samples were mounted in ProLong® Diamond Antifade with DAPI and allowed to cure for 24 h at room temperature. The following antibodies were used at the indicated dilutions: NCX (Swant, R3F1, 1:100), NKA-α1 (Merck Millipore, 05-369, 1:100), NKA-α2 (Merck Millipore, 07-674, 1:100), F(ab')2-Goat anti-Mouse IgG (H+L) secondary antibody (Alexa Fluor 488, Thermo Fisher, A-11017, 1:200), and F(ab')2-goat anti-mouse IgG (H+L) secondary antibody (Alexa Fluor 546, Thermo Fisher, A-11071, 1:200).

All images were captured on an LSM-800 confocal microscope (Carl Zeiss AG, Oberkochen, Germany) equipped with a Plan-Apochromat 63x/1.4 oil immersion lens. Excitation and emission wavelengths were as follows: AF488 (493, 517), AF546 (557, 572). Image resolution was 4096 × 4096 pixels (pixel width 0.041 µm) with a pixel dwell time of 2.06 µs. The Airyscan modality was used for both image acquisition and post-processing.

Cryosectioning, fixation, and imaging of intact myocardium

Rapidly excised ventricular and atrial tissue was positioned in a silicon mould containing Tissue Tek® O.C.T. compound (Sakura® Fintek, Torrance, CA, USA), and submerged in melting 2-methylbutane until frozen. Tissue blocks were trimmed into 10 µm sections at 20°C using a Cryo-Star HM 560 cryostat (Microm International GmbH, Dreieich, Germany).

Sections were transferred to Poly-Prep slides (Merck Life Science, Darmstadt, Germany) and fixed in 4% paraformaldehyde for 8 min at 14 °C. Paraformaldehyde activity was quenched with 100 mmol/L glycine in PBS, and sections were permeabilized with 0.5% Triton X-100 (Merck), both for 15 min at room temperature. Sections were washed with PBS between all steps. Subsequent antibody labelling and Airyscan imaging were performed as described above for isolated cardiomyocytes. T-tubules were labeled in intact cardiac tissue using caveolin-3 antibody (ab2912, Abcam, Cambridge, UK) at 1:100 dilution. For all employed immunolabels, imaging was performed with secondary antibodies alone to exclude the influence of non-specific fluorescence.

Patch-clamp experiments

Both current- and voltage-clamp experiments were performed using 1-2 MΩ pipettes and an Axoclamp-2B amplifier (Axon Instruments, Foster City, CA, USA). pCLAMP software (Axon Instruments) was used to acquire and analyze data.

APs were recorded in bridge-mode, and elicited by 3 ms supra-threshold current steps at 1 Hz. Ca^{2+} transients were simultaneously measured by loading cells with 20 µM fluo-4 AM and recording confocal linescans (LSM 510 microscope, Zeiss), as described previously.[47] Initial AP characterization was performed with a pipette solution contained (in mM) 120 K-aspartate, 0.5 $MgCl_2$, 6 NaCl, 10 HEPES, 10 glucose, 25 KCl, 4 K_2-ATP, 1.9 $CaCl_2$, 1.85 EGTA, and pH=7.2. Free [Ca^{2+}] was calculated to be 10 nM by MaxChelator (https://somapp.ucdmc.ucdavis.edu/pharmacology/bers/maxchelator/CaMgATPEGTA-TS.htm). Cells observed to be electrically stable in control conditions were exposed to simulated hypokalemia by lowering extracellular [K^+] from 5.0 to 2.7 mM. For examination of the effects of intracellular Ca^{2+} buffering, EGTA concentration was set at 60 µM and $CaCl_2$ was removed from the pipette solution. Effects of inhibition of ultra-rapid K^+ current (I_{Kur}) on AP configuration were assessed during rapid application of 50 µmol/L 4-aminopyridine (4-AP). This concentration has been previously shown to almost completely block I_{Kur} while having minimal influence on other currents such as transient outward K^+ current (I_{TO}).[20, 21] Effects of I_{Na} inhibition were assessed by rapid application of 1 µmol/L tetrodotoxin (TTX, Abcam),[15] and effects of triggered Ca^{2+} release during the AP were blocked with 10 mM caffeine. All AP recordings were corrected for liquid junction potentials. AP duration was measured as time from the upstroke to 25, 50, and 75% repolarization (APD_{25}, APD_{50},

APD_{75}), and full duration was defined as repolarization to 5 mV above resting membrane potential. EADs were defined as positive voltage deflections during the downstroke of the action potential repolarization with a minimum amplitude of 2 mV. DADs were defined as minimum 2 mV depolarizing deflections from resting potential.

Membrane currents were recorded in discontinuous voltage-clamp, using a switching rate of 8 kHz. NKA currents were recorded based on a described protocol [6], with a pipette solution containing (mM): Hepes 10, tetraethylammonium chloride 20, L-aspartate 42, EGTA 42, $CaCl_2$ 29.7, Na_2phosphocreatine 5, MgATP 10, NaOH 40, pH=7.2 with CsOH. Cells were bathed in a solution containing (in mM): NaCl 147, $MgCl_2$ 2, EGTA 0.1, D-glucose 5.5, Hepes 5, $BaCl_2$ 2, nicardipine 0.001, KCl 5.0 *or* 2.7, pH=7.4 with NaOH, at 22ºC. From a holding potential of -20 mV, NKA currents were elicited using hyperpolarizing voltage ramps from +70 to -120 mV, and defined as the reduction in current when extracellular K^+ was rapidly removed (Online Figure IA, B). Data were fit with a 5-parameter sigmoid.

K^+ currents were recorded with an intracellular solution containing (in mM): 120 K-aspartate, 0.5 $MgCl_2$, 6 NaCl, 10 HEPES, 10 glucose, 25 KCl, 4 K_2-ATP, 0.06 EGTA, pH=7.2. Extracellular solutions simulating normokalemic and hypokalemic conditions were as above, maintained at 22ºC. Steady-state K^+ currents were measured at the end of 500 ms depolarizing voltage steps from -70 mV to a range of potentials (-120 mV to +60 mV, illustrated in Online Figure IIA). In further experiments, the contribution of I_{TO} to steady-state current was inhibited using a 1 s inactivating voltage step from -70 mV to +50 mV. This was followed by a brief step back to holding potential current, and then a 100 ms test step to a range of potentials (-70 to +150 mV, illustrated in Online Figure IIIA, described in [22]). Previous work has shown that slow recovery of I_{to} from inactivation at room temperature allows better isolation of I_{Kur} in the steady-state current at the end of the test pulse.[22, 42]

NCX activity was examined using the tail current elicited by repolarization following a 100 ms voltage step from -45 to 0 mV (Online Figure V).[48] Each tail current was fit with a double exponential to obtain the second time constant (τ_{slow}), and these values were compared during perfusion with extracellular solutions simulating normo- and hypokalemic conditions, as above. L-type Ca^{2+} currents elicited by the depolarizing step of this protocol were previously reported.[6]

Cellular capacitance was measured by integrating the current elicited by a voltage step from −70 to −80 mV. NKA and K^+ currents are presented normalized to these values, in units of pA/pF.

Western blotting

Western blotting was performed as previously described.[24] Briefly, homogenates of rat left atria and left ventricles were prepared in protein lysis buffer using a TissueLyserII (QIAGEN, Hilden, Germany), and centrifuged (4000 rpm, 10 min, 4 °C). The resultant supernatant was stored at -70 °C. Total protein samples were run on CriterionTM TGXTM pre-cast gels, and transferred to 0.45 µm PVDF membranes (both from Bio-Rad Laboratories, Inc., Hercules, CA, USA). Blots were blocked in non-fat dairy milk in TBS-T and incubated overnight with primary antibody (anti-Kv1.5, APC-004, Alomone, Jerusalum, Israel) with a 1:1000 dilution at 4°C. Blots were then incubated with anti-rabbit horseradish peroxidase-conjugated secondary antibody for 1 h at room temperature, developed with ECL prime (Amersham/GE HealthCare, Buckinghamshire, UK), and visualized on a LAS-4000 (Fujifilm, Tokyo, Japan). Image processing and signal quantification were performed in ImageQuant TL (v2003.03; RRID:SCR_014246) and ImageJ (RRID:SCR_003070), respectively.

PCR analyses

qPCR was performed as described in [23]. Frozen rat right atrial and left ventricular homogenates were defrosted and mRNA was extracted using an RNeasy Mini Kit (Qiagen, Hilden, Germany). qPCR was then performed with TaqMan assays (Applied Biosystems, Foster City, CA) to quantify expression of KCNA5 (Rn00564245_s1 75rxns, ThermoFisher Scientific, Waitham, MA, USA), normalised to the expression of the housekeeping gene Gapdh (Rn99999916_s1, ThermoFisher).

Mathematical modelling

A computational simulation of the time-dependent effects of hypokalemia on Na^+ and Ca^{2+} homeostasis was performed by adapting the model of Terkildsen *et al.*,[25] wherein a set of ordinary differential equations describes the electrophysiology of the rat cardiomyocyte. For the purpose of this study, crosstalk between NCX and NKA activity was simulated by including a new dimensionless parameter NCX_{rev} to scale the intracellular Na^+ concentration (Na_i) sensed by the exchanger:

$$I_{NCX} = \frac{g_{NCX}\left(\mathrm{NCX_{rev}} \times e^{\eta \mathrm{FV/(RT)}} \mathrm{Na_i^3 Ca_o} - e^{(\eta-1)\mathrm{FV/(RT)}} \mathrm{Na_o^3 Ca_i}\right)}{(\mathrm{Na_o^3} + K_{\mathrm{mNa}}^3)(\mathrm{Ca_o} + K_{\mathrm{mCa}})(1 + k_{sat} e^{(\eta-1)\mathrm{FV/(RT)}})}$$

Increasing NCX_{rev} thus effectively augmented the proportion of exchanger activity operating in reverse mode, as expected when NCX is localized closer to NKA and higher local Na^+ levels. Sensitivity analyses were also performed to examine the effects of altered activity of individual ion channels/exchangers: the sodium channel (gNa), sodium-calcium exchanger (gNCX), and sodium-potassium pump (I_{NaKmax}) currents, and the number of L-type Ca^{2+} channel-RyR units. In each case, the prefactor for each ion flux was varied by +/- 5%. The model equations were encoded in the CellML 1.0 standard (https://www.cellml.org) and solved by the Newton method using the CVODE integrator on the Cellular Open Resource platform (COR, version 0.9.31.1409; http://cor.physiol.ox.ac.uk) on a standard desktop computer (16GB, 3.40GHz x 8 processor). Hypokalemia experiments were simulated by instantaneously changing extracellular $[K^+]$ from 5.0 to 2.7 mM. After each modification of the model, steady state was reached by integrating the model equations over 10,000 beats, where the amplitude of the AP became constant typically to within $2e^{-4}$%. The simulation outputs were then analysed in Matlab (R2014b, MathWorks, Natick, MA).

Computational analysis of atrial myocyte electrophysiology was performed using our established human atrial cell model,[26] recently updated with a Markov model of Na^+ current.[14] Experimental voltage recordings were used as inputs in AP-clamp simulations to reveal underlying dynamics of Na^+, Ca^{2+}, and NCX currents. In some simulations, the AP was interrupted at the EAD take-off potential and a voltage step to -30 mV was applied to estimate I_{Na} availability. Further modeling tested effects of varying –dV/dt during the repolarizing phase of the AP, and the influence of membrane hyperpolarization during hypokalemia. The simulations were performed in Matlab using the stiff ordinary differential equation solver ode15s. Model code is available for download at: https://somapp.ucdmc.ucdavis.edu/Pharmacology/bers/ or http://elegrandi.wixsite.com/grandilab/downloads.

Chemicals and reagents

Salts and solution constituents were purchased from Sigma-Aldrich unless stated otherwise. Di-8-ANNEPS (D3167) was dissolved in DMSO plus 20% pluronic acid F-127 (P-6867) (Molecular Probes). All solutions were made using ultrapure water supplied by Milli-Q system (Millipore).

Statistics

All data were tested for normality of distribution using a Shapiro-Wilk test. Normally distributed data were compared with Student's *t*-test or ANOVA with Bonferroni correction for multiple comparisons, as appropriate. Non-normal distributions were examined with a Wilcoxon signed rank test, Mann-Whitney rank sum test, or Kruskal-Wallis analysis on ranks with Dunn's correction for multiple comparisons. Two-factor comparisons were performed with two-way ANOVA with Bonferroni correction; results of post-hoc comparisons are presented in the Online Tables. Differences in proportions were determined by z-test. p values < 0.05 were considered statistically significant. Outliers were defined as values > 3 S.D. from the mean, and excluded. All data were analyzed by Sigmaplot software (Systat Software), and are presented as mean ± SE.

We have not performed nested (mixed model) statistics to address potential differences in cardiomyocytes isolated from different hearts. This should be noted as a statistical weakness of the study. However, since we have employed only normal, inbred rats, it might be expected that differences in basic myocyte physiology between animals are minimal.

ONLINE FIGURES

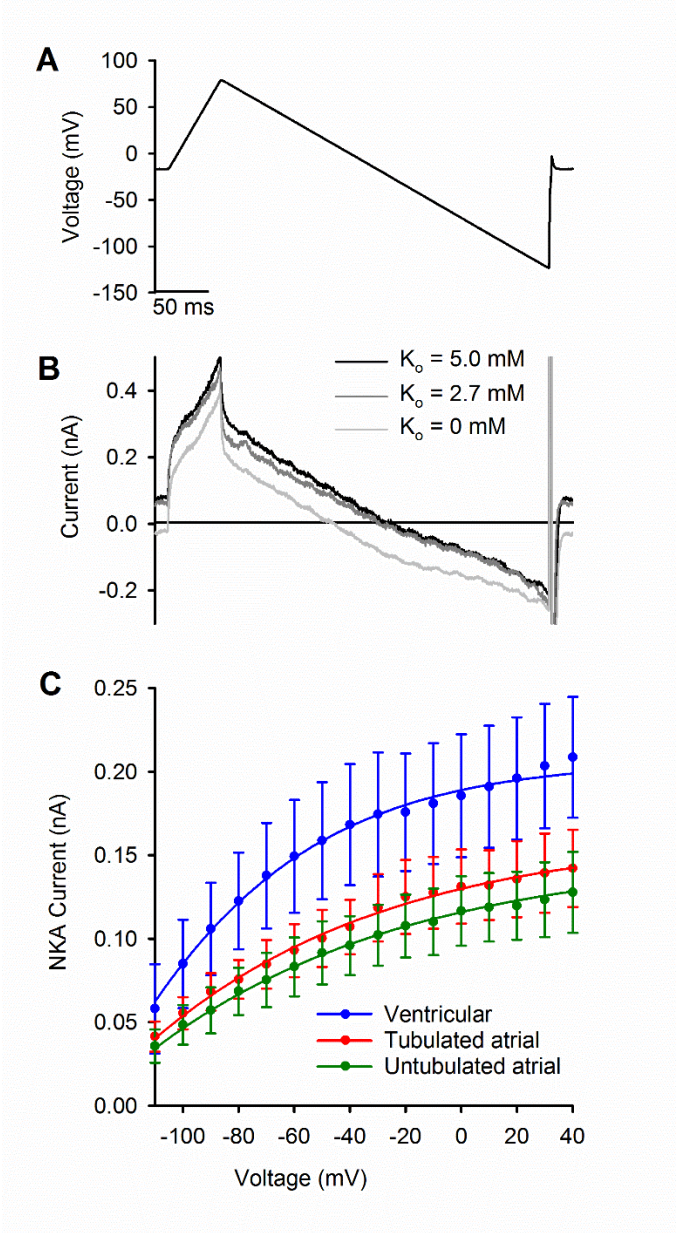

Online Figure I. Recording of NKA currents.
A. NKA currents were measured using a previously described protocol,[6] with hyperpolarizing voltage ramps from +70 to –120 mV. **B.** NKA current was defined as the reduction in current when extracellular [K^+] was rapidly dropped from 5.0 or 2.7 mmol/L to 0. A recording from a representative tubulated atrial myocyte is illustrated. **C.** Mean unnormalized NKA currents under nomokalemic conditions in ventricular mycoytes, tubulated, and untubulated atrial myocytes. n = 10, 7, 9 cells from 4, 4, 5 hearts in ventricular, tubulated atrial, and untubulated atrial cells. **Statistics.** Two-way ANOVA test with Bonferroni correction. Tubulated and untubulated atrial myocyte curves were significantly different from ventricular myocytes (difference in means: $p=4.41 \times 10^{-7}$, $p=2.18 \times 10^{-12}$, respectively; see Online Table I for full results).

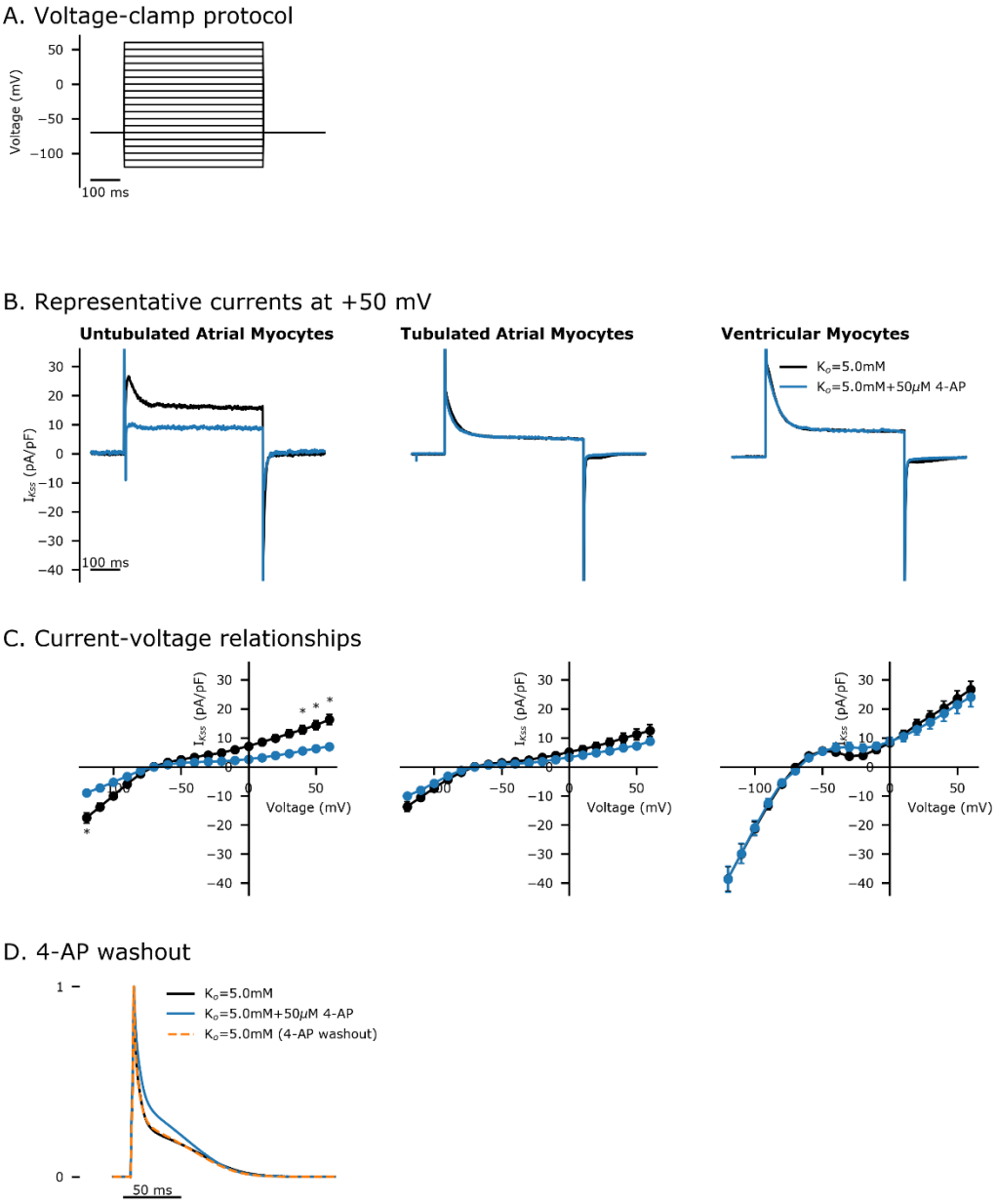

Online Figure II. Recording of steady-state K^+ current.
A. Steady-state K^+ currents were measured at the end of 500 ms depolarizing voltage steps from -70 mV to a range of potentials. Measured changes in steady-state currents during simulated hypokalemia are presented in Fig. 6E and 7F for ventricular and atrial myocytes, respectively. **B.** Treatment with 50 µmol/L 4-AP reduced steady-state currents only in untubulated atrial myocytes, indicating the presence of I_{Kur} exclusively in these cells. **C.** Mean current-voltage relationships in the presence and absence of 4-AP. K_o=5.0: n_{cells}, n_{hearts}= 46, 14 in untubulated atrial; 25, 12 in tubulated atrial; 21, 10 in ventricular myocytes. K_o=5.0+4-AP: n_{cells}, n_{hearts}= 8, 4 in untubulated atrial; 7, 5 in tubulated atrial; 8, 7 in ventricular myocytes. **D.** In agreement with inhibition of I_{Kur}, rapid application of 50 µM 4-AP also reversibly prolonged the AP plateau during K_o=5.0 (n=4 untubulated atrial cells). **Statistics.** Panel C: two-way ANOVA; * = $p<0.05$. See Online Table VI for full results.

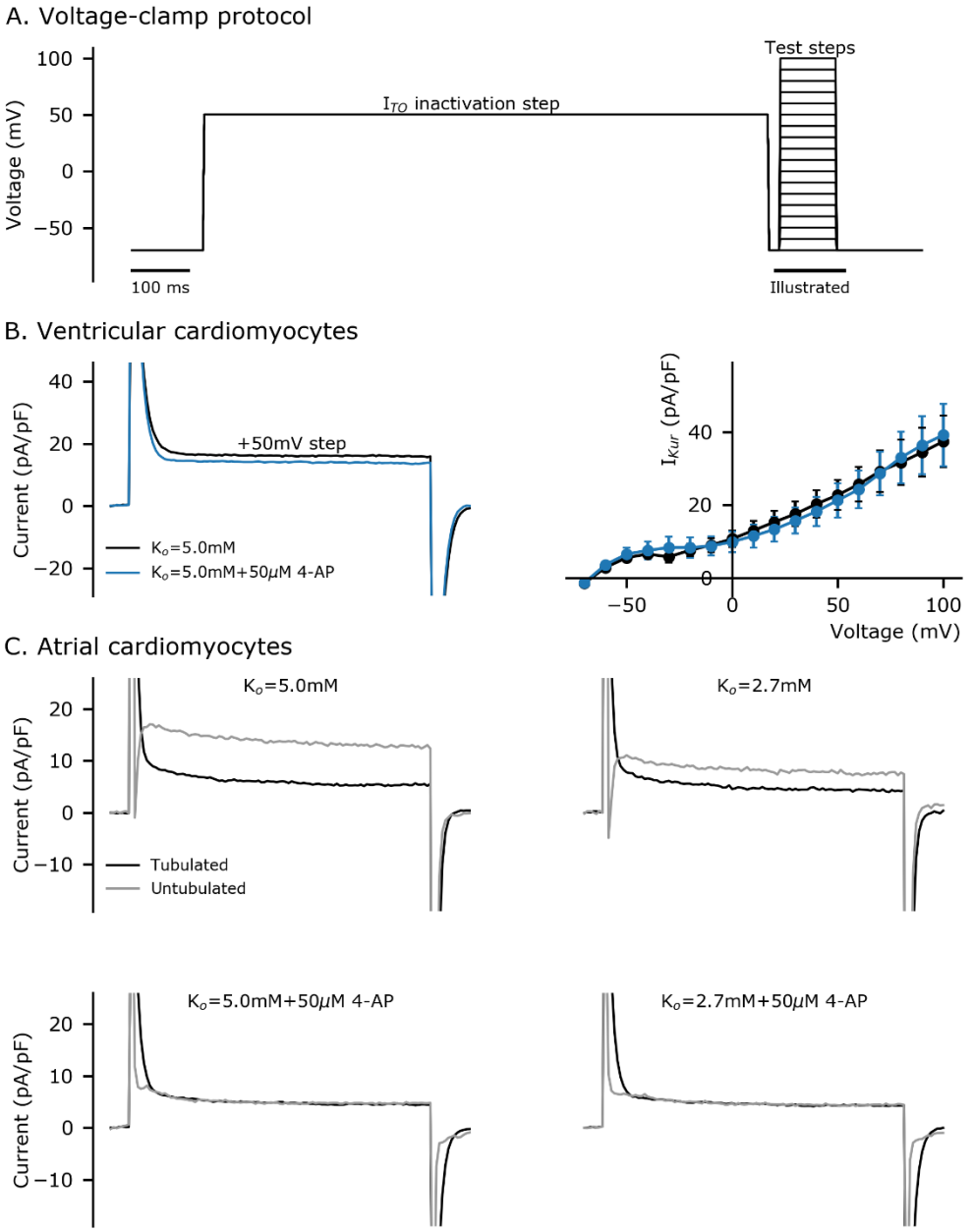

Online Figure III. Recording of ultra-rapid K^+ current (I_{Kur}).
A. To better isolate the I_{Kur} component of steady-state K^+ current, a protocol described in [22] was employed to inactivate I_{TO}. Inactivation was accomplished with a 1 s voltage step from -70 mV to +50 mV, prior to 100 ms test steps from -70 mV to a range of potentials. **B.** When the protocol was employed in ventricular cells, end-of-pulse currents did not include I_{Kur}, as evidenced by a lack of effect of 50 µmol/L 4-AP. n= 18, 7 from 10, 6 hearts in K_o=5.0, K_o=5.0 + 4-AP. **C.** Untubulated atrial myocytes exhibited larger end-of-pulse currents than tubulated cells, and 4-AP treatment revealed that this difference was due to the presence of I_{Kur} (see Fig. 7G for mean data). **Statistics.** Panel B: two-way ANOVA; no significant difference in means (p=0.981), and no interaction with voltage (p=1.000).

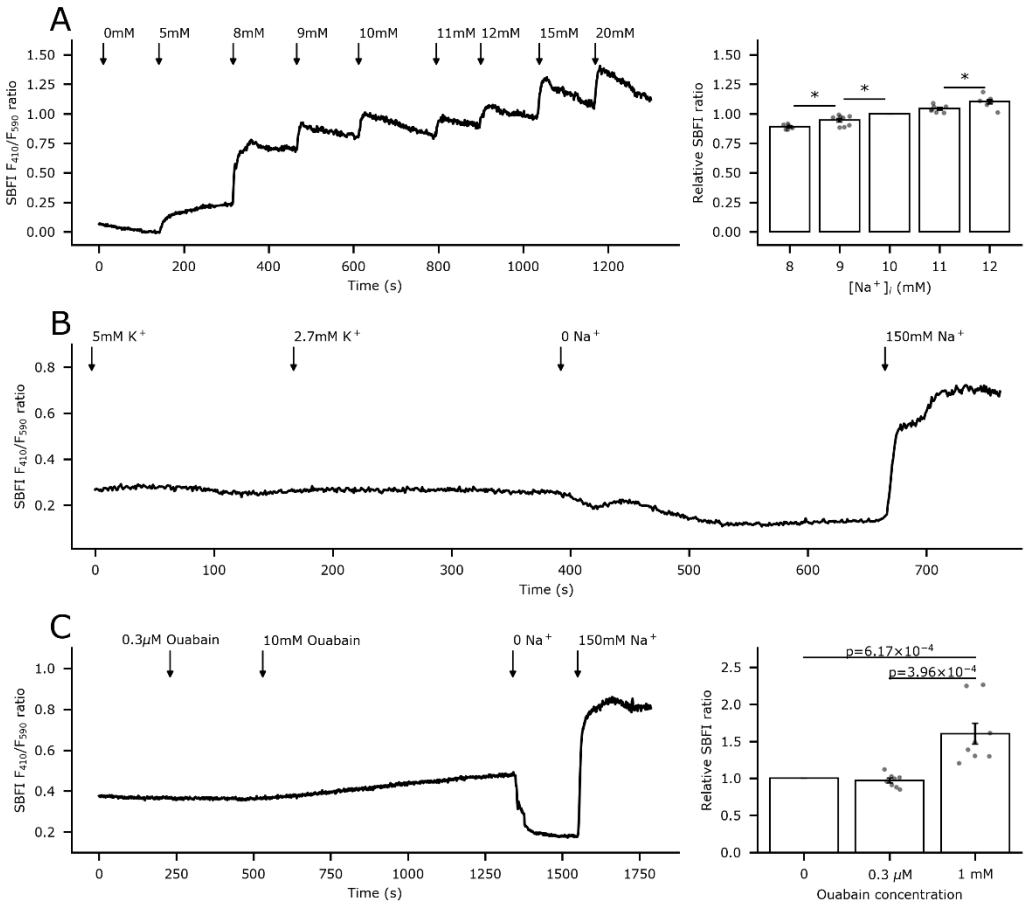

Online Figure IV. Assessment of intracellular [Na^+] by SBFI. Intracellular [Na^+] was recorded in cardiomyocytes incubated with SBFI AM. **A.** To establish the sensitivity of this technique, rat ventricular cardiomyocytes treated with ionophores (see methods) were perfused with solutions containing progressively increasing Na^+ concentrations in the physiological range. Resulting stepwise and significant increases in SBFI ratio demonstrated a minimum detection threshold of 1 mM Na^+ in the physiological range (n_{cells}= 7 from 4 hearts; data normalized to 10 mM Na^+). **B.** In field-stimulated cardiomyocytes, SBFI ratios were recorded during simulated hypokalemia, with reduction of extracellular [K^+] from 5.0 to 2.7 mmol/L. A representative ventricular myocyte is illustrated, with subsequent permeabilization and exposure to 0 and saturating 150 mmol/L Na^+. Mean data are presented in Figure 4B. **C.** SBFI ratio was significantly increased during treatment with high-dose (1 mmol/L) but not low-dose (0.3 µmol/L umol) ouabain (n_{cells} = 8 from 3 hearts). **Statistics.** Panel A: one-way repeated measures ANOVA with Bonferroni correction; difference in means: $p = 2.49x10^{-10}$; see Online Table VII for full results. Panel C: one-way repeated measures ANOVA; difference in means: $p = 2.49x10^{-10}$. * = $p<0.05$.

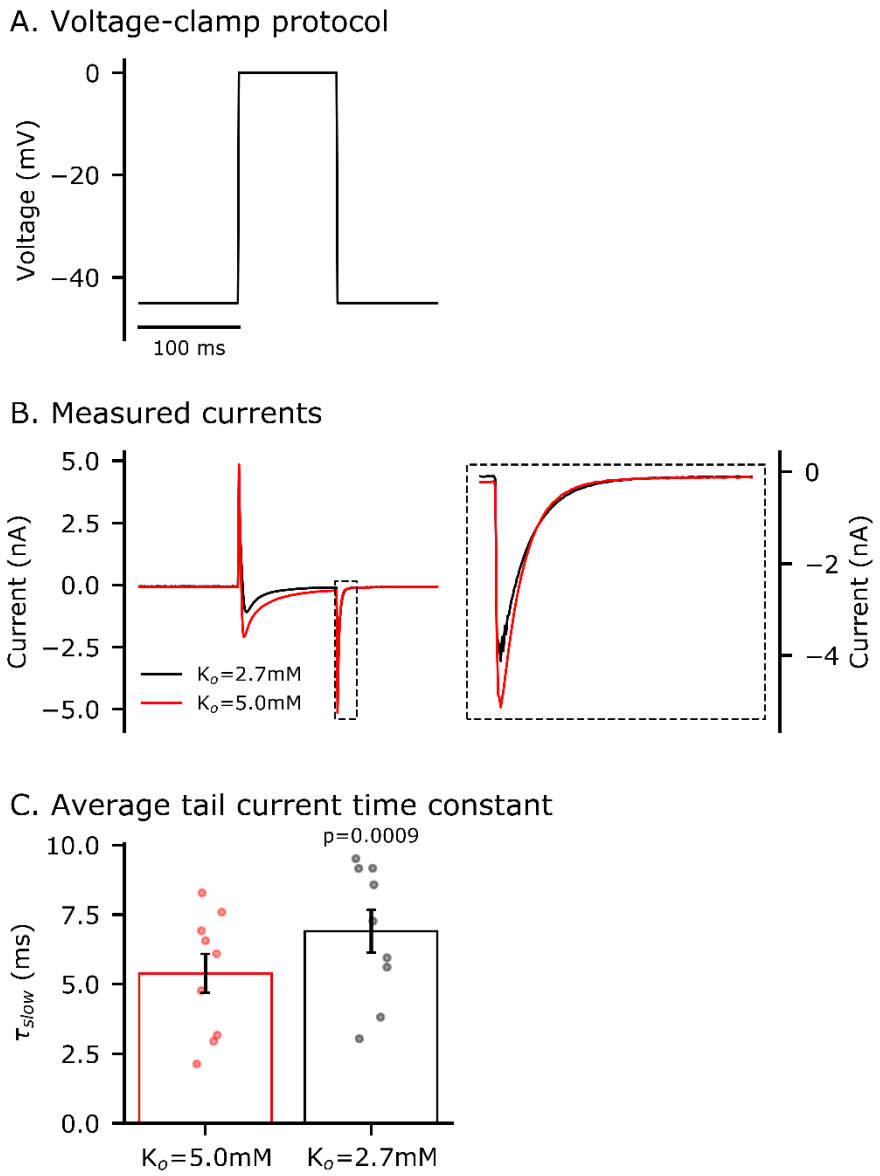

Online Figure V. Hypokalemia slows Ca^{2+} removal by NCX in ventricular myocytes. Changes in NCX activity during hypokalemia were assessed in patch-clamped ventricular myocytes. A voltage step from -45 to 0 mV (**A**) was used to elicit L-type Ca^{2+} current (**B**), as described in [6]. The tail current triggered by repolarization to the holding potential (enlarged in right panel of **B**) was used to assess NCX current.[48] Reduced magnitude of L-type Ca^{2+} current during hypokalemia (see also [6]) was matched by reduced magnitude of the repolarizing tail current. Double exponential fits of the tail current further revealed an increase in the second time constant (τ_{slow}, **C**), consistent with slowed NCX-mediated Ca^{2+} extrusion during hypokalemia. n_{cells} = 9 from 6 hearts. **Statistics:** paired t-test.

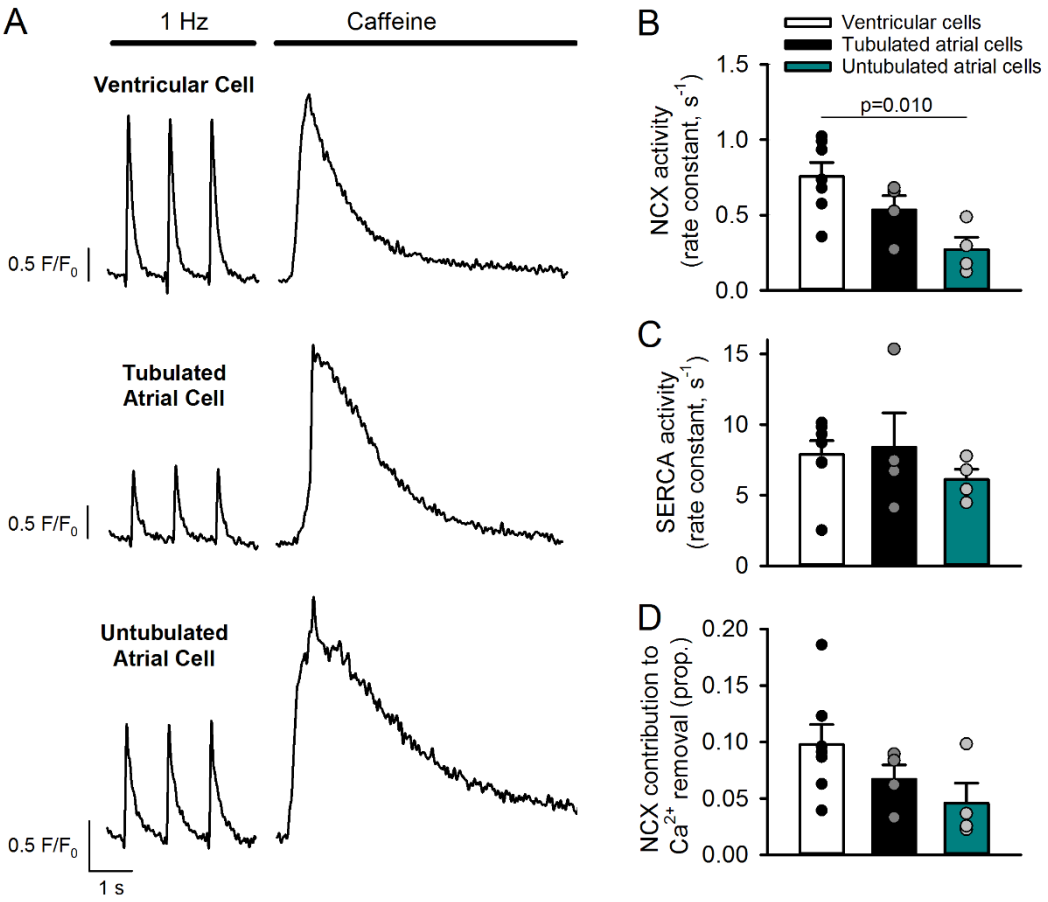

Online Figure VI. Assessment of SR Ca^{2+} content and Ca^{2+} fluxes.
A. SR content was assessed by rapidly applying 10 mmol/L caffeine, after steady-state electrical pacing at 1 Hz. **B.** NCX activity was estimated by fitting the decay of the caffeine-elicited Ca^{2+} transient, to obtain a rate constant (1/Tau). **C.** SERCA activity was calculated as the difference in rate constant measured during the decay of the caffeine and 1 Hz transients.[49] **D.** The proportional NCX contribution to Ca^{2+} decay was assessed by comparing the SERCA rate constant to the overall rate of Ca^{2+} extrusion during 1 Hz pacing. n_{cells} =7, 4, 4; n_{hearts} =4, 4, 4 hearts in ventricular, tubulated atrial, untubulated atrial cells. **Statistics:** one-way ANOVA with Bonferroni correction. Difference in means: p = 0.011, 0.559, 0.141 in Panels A, B, and C, respectively.

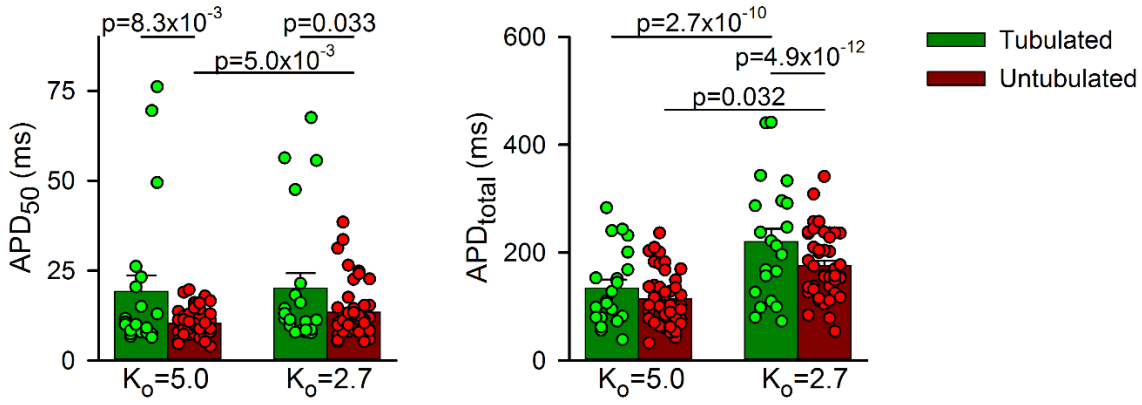

Online Figure VII. Assessment of AP configuration in atrial cardiomyocytes.
Mean AP duration at 50% repolarization (APD_{50}) and at full length (APD_{total}, measured at repolarization to 5 mV above resting membrane potential). APD_{75} measurements are presented in Figure 7D. **Statistics:** Two-way repeated measures ANOVA with Bonferroni correction. Difference in means for APD_{50}: p=0.0134 for tubulated vs untubulated, p=0.0302 for K_o=5.0 vs K_o=2.7. Difference in means for APD_{total}: p=0.0698 for tubulated vs untubulated, $p=1.32x10^{-15}$ for K_o=5.0 vs K_o=2.7. Tubulated cells = 21 from 12 hearts, untubulated cells = 48 from 20 hearts.

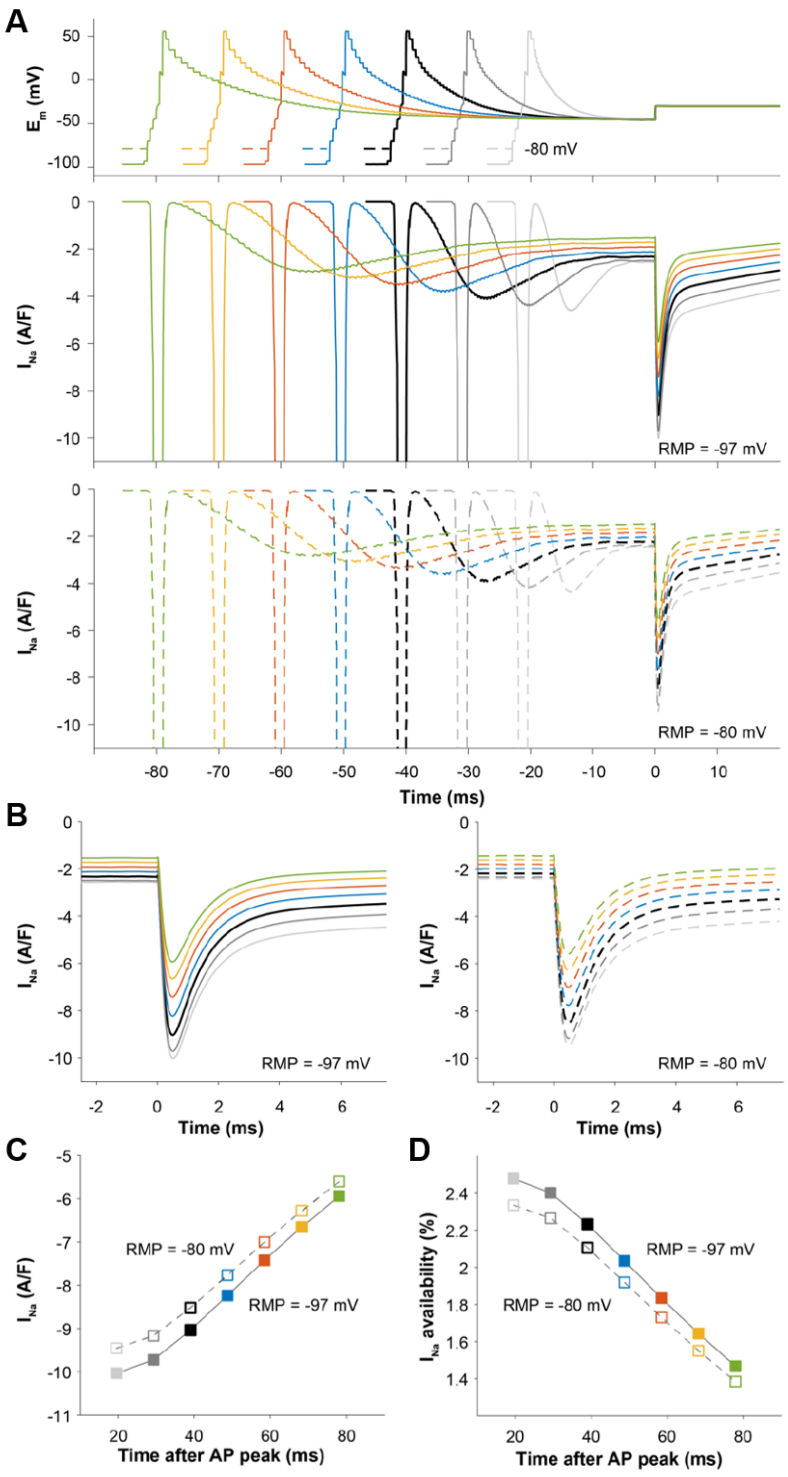

Online Figure VIII. Assessment of Na^+ current available to drive phase-3 EADs. Inclusion of AP waveforms from an untubulated atrial myocyte in a mathematical model of the human atrial cardiomyocyte linked phase-3 EADs to reactivation of non-equilibrium Na^+ current (Figure 7I). **A.** To estimate the I_{Na} available before the onset of these events, the AP clamp was interrupted at the EAD take-off potential, ie. the point where dV/dt = 0, and a voltage step to -30 mV was applied to elicit maximal current. To examine the role of AP duration, the rate of membrane repolarization was accelerated or slowed in a stepwise manner relative to the experimental recording (black line). The influence of membrane

hyperpolarization during hypokalemia, which decreased resting membrane potential from -80 to -97 mV, was assessed by comparing with simulations where this change was offset (dotted lines). **B.** Enlarged tracings of the triggered currents. **C.** Peak current measurements. **D.** I_{Na} values normalized to the current elicited when the voltage step was applied from the resting membrane potential, to obtain the current fraction available at this stage of repolarization. For the representative AP recording employed (black lines and dot), available I_{Na} was ≈2.2% of total current. As the repolarization was slowed, I_{Na} availability steadily declined. In the absence of membrane hyperpolarization during hypokalemia, I_{Na} availability was lower at all AP durations tested.

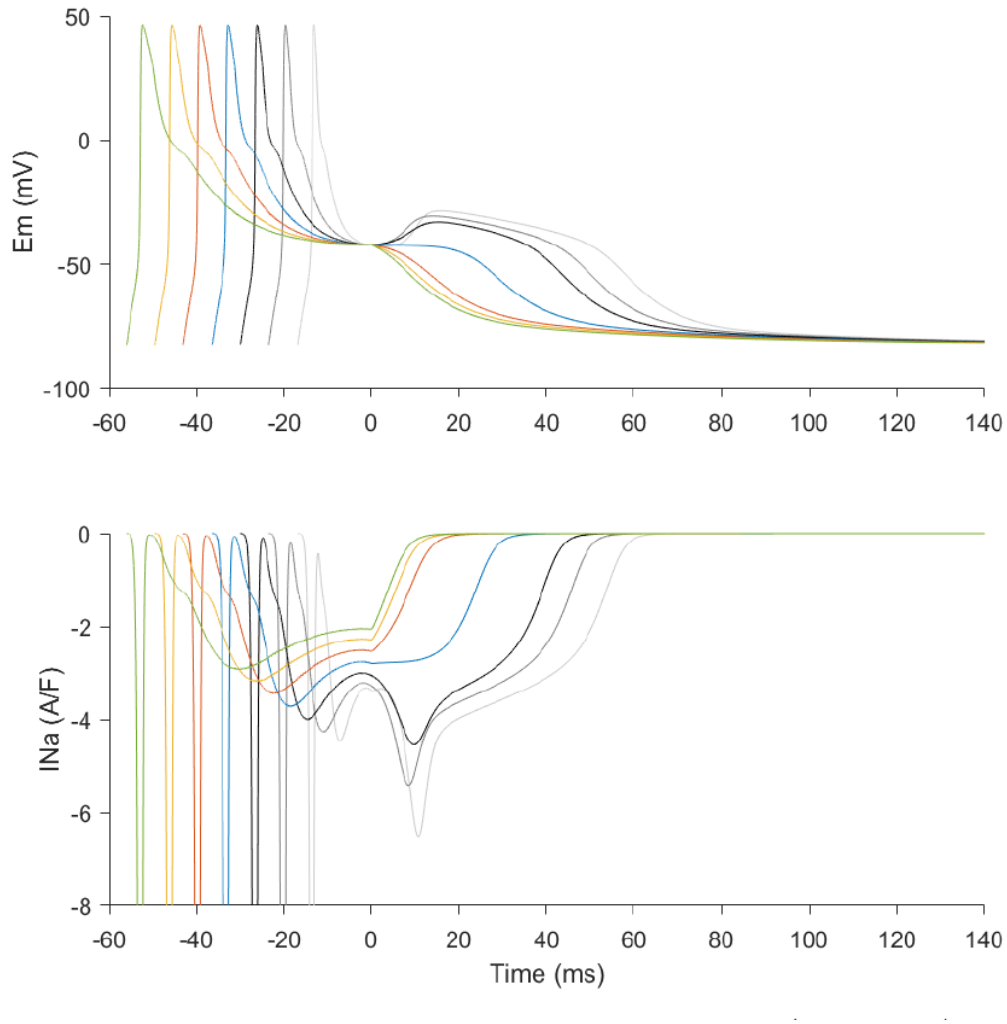

Online Figure IX. I_{Na}-dependent phase-3 EADs require brief action potential configuration. We employed a representative human atrial AP trace modeled in previous work[14] as a voltage-clamp stimulus, until the point of repolarization where dV/dt = 0. When the voltage stimulus was halted, the baseline AP configuration (black line) developed an I_{Na}-dependent EAD. Shortening the AP voltage command induced larger I_{Na} and EADs, while lengthening the AP inhibited I_{Na} reactivation and EAD generation. An I_{Na}-driven EAD required that the time from the AP peak to the take-off potential was less than ≈30 ms.

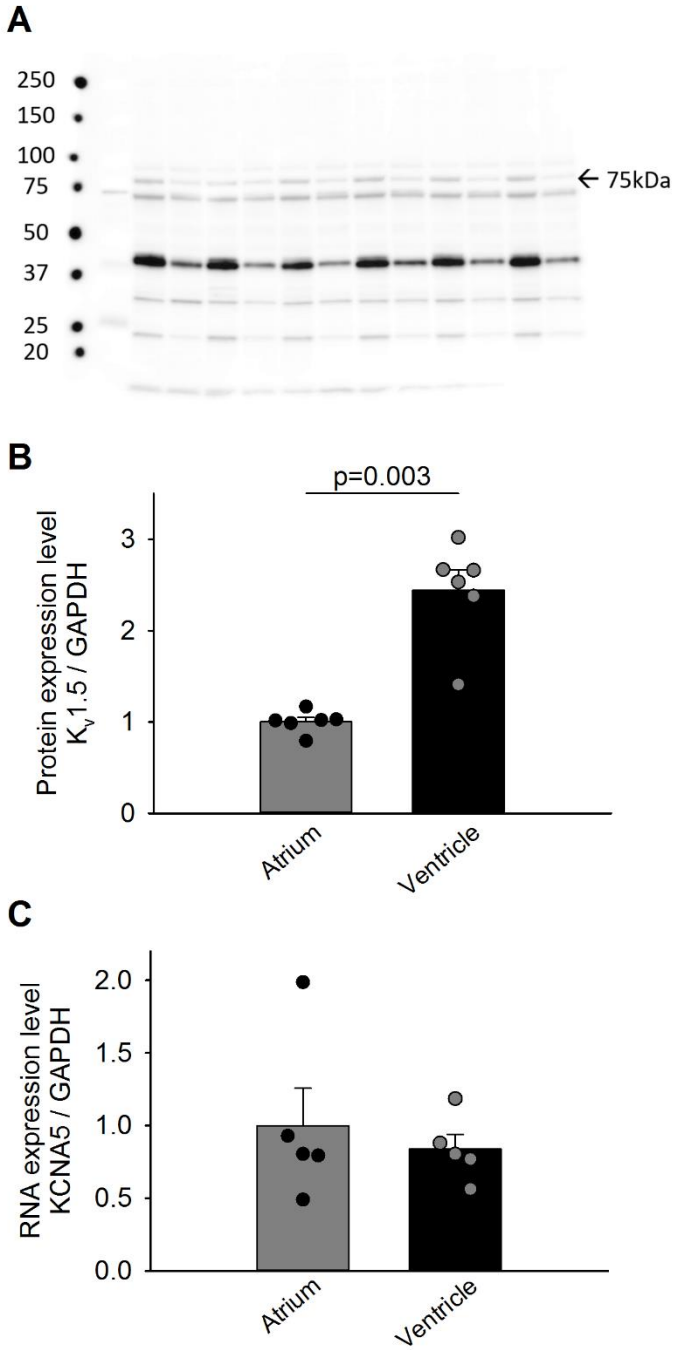

Online Figure X. Expression of K_v1.5 / KCNA5 in rat ventricle and atrium.
A. Western blotting performed on homogenates of rat left atria and left ventricles showed robust expression of K_v1.5, the channel linked to I_{Kur}. Lanes are alternating ventricle and atria, from left. **B.** Quantification of band density at 75 kDa and normalization to atrial values (n_{hearts} = 6). **C.** qPCR analysis of KCNA5, the gene encoding K_v1.5, revealed similar RNA levels in right atrium and left ventricle (n_{hearts} = 5). **Statistics:** paired t-test.

ONLINE TABLES

	Ventricular vs tub atrial cells	Ventricular vs untub atrial cells	Tub vs untub atrial cells
Difference in means	* 4.41E-7	* 2.18E-12	0.385
Within -110 mV	1.000	1.000	1.000
-100 mV	0.785	0.933	1.000
-90 mV	0.580	0.530	1.000
-80 mV	0.479	0.401	1.000
-70 mV	0.251	0.327	1.000
-60 mV	0.201	0.285	1.000
-50 mV	0.188	0.268	1.000
-40 mV	0.136	0.236	1.000
-30 mV	0.137	0.246	1.000
-20 mV	0.178	0.418	1.000
-10 mV	0.150	0.447	1.000
0 mV	0.170	0.400	1.000
10 mV	0.137	0.367	1.000
20 mV	0.105	0.296	1.000
30 mV	0.0807	0.242	1.000
40 mV	0.0765	0.221	1.000

Online Table I. Statistical test results (p values) from comparisons of NKA current in ventricular and atrial myocytes (two-way ANOVA). There was no significant interaction with voltage (p=0.682). Mean data ± SE are presented in Online Figure IC. * = $p < 0.05$.

	K_o=5.0 vs 2.7 mM within ventricular cells	K_o=5.0 vs 2.7 mM within tub atrial cells	K_o=5.0 vs 2.7 mM within untub atrial cells
Test	Two-way RM ANOVA	Two-way RM ANOVA	Two-way RM ANOVA
Difference in means	* 0.0231	* 8.49E-04	* 8.34E-03
Interaction w/ voltage	0.997	1.000	0.847
Within -110 mV	* 0.0500	0.113	0.256
-100 mV	0.0504	0.0608	0.178
-90 mV	* 0.0396	* 0.0165	0.359
-80 mV	0.0516	* 0.0388	0.103
-70 mV	* 0.0414	0.0633	0.178
-60 mV	* 0.0257	0.0519	0.166
-50 mV	* 0.0226	* 0.0181	* 0.0349
-40 mV	* 0.0174	* 0.0280	* 0.0268
-30 mV	* 0.0180	* 0.0137	* 0.0235
-20 mV	* 0.0199	* 5.45E-03	* 4.83E-03
-10 mV	* 0.0245	* 0.0445	* 9.84E-03
0 mV	* 0.0222	* 0.0340	* 6.28 E-03
10 mV	* 0.0145	0.0970	* 9.21 E-03
20 mV	* 0.0246	0.155	* 0.0190
30 mV	* 0.0232	0.124	* 0.0220
40 mV	* 0.0436	0.142	* 0.0445

Online Table II. Statistical test results (p values) from measurements of NKA current density. Mean data ± SE are presented in Figure 4A. * = $p < 0.05$.

	K_o=5.0 vs 2.7 mM within ventricular cells
Test	Two-way RM ANOVA
Difference in means	* 0.0102
Interaction w/ voltage	* 4.63E-19
Within -120 mV	* 4.15E-15
-110 mV	* 1.24E-12
-100 mV	* 1.13E-09
-90 mV	* 2.36E-06
-80 mV	* 2.38E-03
-70 mV	0.149
-60 mV	0.849
-50 mV	0.517
-40 mV	0.484
-30 mV	0.727
-20 mV	0.874
-10 mV	0.978
0 mV	0.873
10 mV	0.663
20 mV	0.469
30 mV	0.317
40 mV	0.246
50 mV	0.238

Online Table III. Statistical test results (p values) from measurements of steady-state K^+ current in ventricular cells. Mean data ± SE are presented in Figure 6E. * = $p < 0.05$.

	Tub vs untub cells within K_o=5.0 mM	Tub vs untub cells within K_o=2.7 mM	K_o=5.0 vs 2.7 mM within tub cells	K_o=5.0 vs 2.7 mM within untub cells
Test	Two-way ANOVA	Two-way ANOVA	Two-way RM ANOVA	Two-way RM ANOVA
Difference in means	0.436	0.0660	* 3.00E-03	* 7.07E-04
Interaction w/ voltage	* 0.0393	* 5.21 E-04	* 1.72E-16	* 6.36E-45
Within -120 mV	0.0794	0.0936	* 2.15E-04	* 1.62E-10
-110 mV	0.171	0.243	* 4.54E-04	* 2.52E-09
-100 mV	0.238	0.385	* 0.0113	* 1.59E-06
-90 mV	0.476	0.676	0.145	* 2.37E-03
-80 mV	0.852	0.830	0.385	0.237
-70 mV	0.992	0.994	0.944	0.924
-60 mV	0.815	0.878	0.710	0.401
-50 mV	0.709	0.706	0.477	0.222
-40 mV	0.618	0.584	0.424	0.176
-30 mV	0.492	0.470	0.413	0.109
-20 mV	0.537	0.315	0.286	0.246
-10 mV	0.419	0.206	0.318	0.251
0 mV	0.345	0.156	0.329	0.211
10 mV	0.258	0.0821	0.260	0.176
20 mV	0.191	0.0537	0.263	0.133
30 mV	0.106	* 0.0347	0.339	0.0631
40 mV	0.0869	* 0.0146	0.226	0.0694
50 mV	0.0546	* 6.83E-03	0.148	* 0.0254
60 mV	* 0.0341	* 2.55E-03	0.153	* 0.0267

Online Table IV. Statistical test results (p values) from measurements of steady-state K^+ current in atrial cells. Mean data ± SE are presented in Figure 7F. * = $p < 0.05$.

	Tub vs untub cells within K_o=5.0 mM	Tub vs untub cells within K_o=2.7 mM	K_o=5.0 vs 2.7 mM within tub cells	K_o=5.0 vs 2.7 mM within untub cells
Test	Two-way ANOVA	Two-way ANOVA	Two-way RM ANOVA	Two-way RM ANOVA
Difference in means	* 1.57E-10	* 1.42E-65	* 1.81E-03	0.468
Interaction w/ voltage	0.978	0.566	* 3.81E-06	0.992
Within -70 mV	0.906	0.987	0.991	0.870
-60 mV	0.896	0.813	0.519	0.849
-50 mV	0.753	0.620	0.290	0.771
-40 mV	0.534	0.470	0.332	0.732
-30 mV	0.535	0.376	0.228	0.829
-20 mV	0.357	0.320	0.202	0.592
-10 mV	0.343	0.326	0.186	0.532
0 mV	0.220	0.207	0.165	0.526
10 mV	0.224	0.204	0.182	0.566
20 mV	0.148	0.123	0.177	0.622
30 mV	0.129	0.0675	0.130	0.813
40 mV	0.0756	0.0917	0.129	0.391
50 mV	* 0.0445	0.0770	0.0845	0.234
60 mV	0.0971	* 0.0221	* 6.30E-03	0.663
70 mV	0.0676	* 0.0270	* 1.38E-03	0.272
80 mV	0.0990	* 0.0167	* 3.16E-04	0.423
90 mV	0.0721	* 0.0135	* 1.55E-04	0.312
100 mV	0.151	* 5.17E-03	* 8.32E-07	0.476
+4-AP				
Test	Two-way ANOVA	Two-way ANOVA	Two-way ANOVA	Two-way ANOVA
Difference in means	0.243	* 2.95E-03	* 3.88E-05	0.711
Interaction w/ voltage	1.000	1.000	0.995	1.000
Within -70 mV	0.883	0.976	0.908	0.955
-60 mV	0.976	0.899	0.744	0.682
-50 mV	0.770	0.680	0.879	0.987
-40 mV	0.879	0.702	0.765	0.989
-30 mV	0.931	0.752	0.537	0.781
-20 mV	0.949	0.606	0.336	0.805
-10 mV	0.891	0.489	0.346	0.997
0 mV	0.813	0.482	0.326	0.954
10 mV	0.940	0.528	0.397	0.972
20 mV	0.704	0.438	0.247	0.921
30 mV	0.728	0.382	0.222	0.909
40 mV	0.836	0.45	0.322	0.941
50 mV	0.698	0.323	0.13	0.986
60 mV	0.530	0.172	* 0.0648	0.765
70 mV	0.537	0.227	0.146	0.643
80 mV	0.527	0.273	2.214	0.683
90 mV	0.417	0.228	2.568	0.631
100 mV	0.256	0.28	* 0.0907	0.559

Online Table V. Statistical test results (p values) from measurements of steady-state K^+ current after inhibition of I_{TO}. Mean data ± SE are presented in Figure 7G, top and bottom panels.
* = $p < 0.05$.

	Untubulated atrial cells	Tubulated atrial cells	Ventricular cells
Test	Two-way ANOVA	Two-way ANOVA	Two-way ANOVA
Difference in means	0.473	0.176	0.887
Interaction w/ voltage	* 2.07E-09	* 0.025	1.000
Within -120 mV	* 0.0153	0.332	0.989
-110 mV	0.0647	0.506	0.982
-100 mV	0.183	0.651	0.957
-90 mV	0.450	0.748	0.926
-80 mV	0.741	0.853	0.947
-70 mV	0.962	0.977	0.851
-60 mV	0.837	0.917	0.921
-50 mV	0.749	0.879	0.993
-40 mV	0.624	0.835	0.819
-30 mV	0.512	0.786	0.633
-20 mV	0.416	0.712	0.710
-10 mV	0.286	0.693	0.843
0 mV	0.208	0.636	0.952
10 mV	0.132	0.581	0.916
20 mV	0.0887	0.541	0.807
30 mV	0.0541	0.451	0.777
40 mV	* 0.0395	0.393	0.776
50 mV	* 0.0234	0.299	0.753
60 mV	* 9.23E-03	0.300	0.695

Online Table VI. Statistical test results (p values) comparing measurements of steady-state K^+ currents ± 4-AP. Mean data ± SE are presented in Online Figure IIC. * = $p < 0.05$.

	$[Na^+]_i$ (mM)				
	8	9	10	11	12
8		* 0.0391	* 7.27E-07	* 2.47E-07	* 5.80E-10
9			* 0.0149	* 1.26E-04	* 6.18E-08
10				0.208	* 3.4E-05
11					* 0.0433
12					

Online Table VII. Two-way repeated measures ANOVA test results (p values) comparing changes in SBFI ratio with known increases in $[Na^+]_i$. Overall p value = 2.49E-10. Mean data ± SE are presented in Online Figure IVA. * = $p < 0.05$.